Bis(1,2-bis(diphenylphosphino)ethane)tungsten(0) Complexes Containing Electron-Saturated Metal Centers and Singly-Coordinated Bridging Ligands

Cuie Hu, William C. Hodgeman, and Dennis W. Bennett*

Department of Chemistry, University of Wisconsin−Milwaukee, Milwaukee, Wisconsin 53201

Received July 7, 1995[⊗]

Reaction of 1,4-diisocyanobenzene or 4-isocyanobenzonitrile with *trans*-W(N$_2$)$_2$(DPPE)$_2$ (DPPE = 1,2-bis-(diphenylphosphino)ethane) produced *cis*-WL$_2$(DPPE)$_2$, where L = 1,4-diisocyanobenzene or 4-isocyanoben-zonitrile. *cis*-(CNC$_6$H$_4$NC)$_2$W(DPPE)$_2$ crystallizes in the triclinic space group $P\bar{1}$, with a = 12.848(3) Å, b = 13.596(3) Å, c = 19.072(3) Å, α = 78.99(2)°, β = 70.66(2)°, γ = 65.26(2)°, V = 2849.8(11) Å^3, and Z = 2. *cis*-(NCC$_6$H$_4$NC)$_2$W(DPPE)$_2$ crystallizes in the triclinic space group $P\bar{1}$, with a = 12.712(3) Å, b = 13.700(3) Å, c = 19.109(3) Å, α = 77.91(2)°, β = 70.63(2)°, γ = 64.76(2)°, V = 2830.7(13) Å^3, and Z = 2. Both compounds possess a distorted octahedral geometry about the metal center, with the two isocyanide ligands *cis* to one another. The isocyanide ligands are substantially bent along the CNC axis of the isocyanide group coordinated to tungsten. For the complex containing the symmetric ligand, CNC$_6$H$_4$NC, the mean CNC angle for the coordinated end of the isocyanide is 139.1(11)°, the average W−C bond length is 1.86(1) Å, and the C≡N bond lengths have a mean value of 1.30(2) Å. These data indicate substantial back-donation from an electron-saturated tungsten atom. This is supported spectroscopically, with substantial shifts to lower wavenumbers for the C−N stretching frequencies of the coordinated isocyanide groups. Similar trends are observed in *cis*-(NCC$_6$H$_4$NC)$_2$W(DPPE)$_2$. Both compounds contain electron-rich metals surrounded by large ligands which apparently protect the metals from atmospheric oxidation. The isocyanide ligands in both complexes contain a second coordinating group pointing away from the metal into the environment surrounding the molecules, providing the potential for polymetallic complexes containing metals in a variety of oxidation states.

Introduction

In studying the reactivity of transition metal complexes it is often difficult to separate electronic from steric effects when changes are made which structurally alter the local environment of the metal through ligand substitution. In principle, it is possible to decouple these effects by modifying the ligands themselves, usually relying on electronic communication between a functional group on an aromatic ligand and the metal to which the ligand is bonded. The incorporation of a second transition metal complex as the "functional group" is especially useful in this regard, since transition metals are capable of supporting large variations in charge density. It is therefore possible to modify ligands on one metal center and observe their electronic effects on a second without altering the coordination geometry of the second metal.

In previous work we have shown that diisocyanide bridging ligands are capable of mediating electronic communication between metal centers, and that significant modifications in the properties of one metal can be induced by another metal in a markedly different oxidation state.[1] In work designed to create tunable bimetallic catalysts, we have synthesized complexes of the form (CO)$_4$LWCNPhNCWOCl$_4$. These complexes are extremely susceptible to oxidation, and subsequent loss of CO. Because of this we set out to synthesize similar complexes containing W(0) encompassed by ligands much less susceptible to dissociation. This paper describes the first step in this process: the synthesis and characterization of electron-rich W(0) complexes surrounded by protective chelating ligands and containing two isocyanide or nitrile groups with available lone pairs for attachment to other transition metal complexes.

Experimental Section

General Reagents and Procedures. 1,4-Phenylenediamine was purchased from Fluka Chemica; 1-amino-4-cyanobenzene was purchased from Eastman Kodak Company; 1,2-bis(diphenylphosphino)-ethane was supplied by Strem Chemicals, Inc.; Tungsten(VI) chloride and PPh$_3$ were purchased from Aldrich Chemical Company. Solvents were purchased from VWR Scientific. *trans*-W(N$_2$)$_2$(DPPE)$_2$ was prepared according to literature procedures,[2] as were CNC$_6$H$_4$NC, and NCC$_6$H$_4$NC.[3] All reactions were performed under an atmosphere of dry and oxygen-free nitrogen; all solvents were deoxygenated and dried by distilling from Na−benzophenone or P$_2$O$_5$.

IR spectra were recorded as KBr pellets using a Nicolet MX-1 FT-IR spectrometer. ^{31}P NMR spectra were recorded on a Bruker WM-250 MHz NMR spectrometer with 85% H$_3$PO$_4$ as the external reference. X-ray data were collected on a Picker diffractometer using PCXTL.[4]

Synthesis of *cis*-(CNC$_6$H$_4$NC)$_2$W(DPPE)$_2$. W(N$_2$)$_2$(DPPE)$_2$ (0.160 g, 0.154 mmol) and CNC$_6$H$_4$NC (0.0791 g, 0.617 mmol) were stirred in 80 mL of toluene for 18 h under constant irradiation from a single 60 W incandescent tungsten filament source. The solid was filtered off and the volume of the solvent was reduced to 10 mL. Hexane (10 mL) was added to precipitate the bimetallic complex N$_2$(DPPE)$_2$-WCNC$_6$H$_4$NCW(DPPE)$_2$N$_2$.[5] Addition of hexane (15 mL) to the supernatant gave dark-red crystals of the monometallic species, *cis*-(CNC$_6$H$_4$NC)$_2$W(DPPE)$_2$. The compound was further purified by recrystallization from 1:2 toluene/hexane (32% yield). Anal. Calcd for C$_{68}$H$_{56}$N$_4$P$_4$W: C, 66.03; H, 4.56; N, 4.53. Found: C, 66.55; H, 4.47; N, 5.05. ^{31}P NMR δ(ppm): 32.3 d, 47.8 d. IR (cm^{-1}): ν_{NC}, 2120 s, 1945 s.

Synthesis of *cis*-(NCC$_6$H$_4$NC)$_2$W(DPPE)$_2$. The complex was prepared in an identical manner to *cis*-(CNC$_6$H$_4$NC)$_2$W(DPPE)$_2$ by

---

* Author to whom correspondence should be addressed.
[⊗] Abstract published in *Advance ACS Abstracts,* February 15, 1996.
(1) Grubisha, D. S.; Rommel, J. S.; Lane, T. M.; Tysoe, W. T.; Bennett, D. W. *Inorg. Chem.* **1992,** 31, 5022.

(2) Dilworth, J. R.; Richards, R. L. *Inorg. Synth.* **1980,** 119.
(3) (a) Schenk, W. A. *J. Organomet. Chem.* **1976,** 117, C97. (b) Ugi, I.; Fetzer, U.; Eholzer, U.; Knupfer, H.; Offerman, K. *Angew. Chem., Int. Ed. Engl.* **1965,** 4, 472.
(4) Weinrach, J. B.; Bennett, D. W. *J. Appl. Cryst.* **1991,** 24, 91.
(5) A description of the synthesis and characterization of a series of bimetallics, of which this complex is representative, is currently in preparation for publication.

Table 1. Crystallographic Data for $W(N_2)_2L_2$, $(CNC_6H_4NC)_2WL_2$, and $(NCC_6H_4NC)_2WL_2$ (L = DPPE)

	$W(N_2)_2L_2$	$(CNC_6H_4NC)_2WL_2$	$(NCC_6H_4NC)_2WL_2$
formula	$C_{52}H_{48}N_4P_4W$	$C_{68}H_{56}N_4P_4W$	$C_{68}H_{56}N_4P_4W$
molar mass	1036.85	1236.47	1236.47
cryst syst	triclinic	triclinic	triclinic
space group	$P\bar{1}$	$P\bar{1}$	$P\bar{1}$
a, Å	10.875(2)	12.848(3)	12.712(3)
b, Å	12.384(1)	13.596(3)	13.700(3)
c, Å	17.688(3)	19.072(3)	19.109(6)
α, deg	89.44(1)	78.99(2)	77.91(2)
β, deg	81.73(1)	70.66(2)	70.63(2)
γ, deg	79.47(1)	65.26(2)	64.76(2)
V, Å^3	2317.3(6)	2849.8(11)	2830.7(13)
Z	2	2	2
d_{calc}, g cm^{-3}	1.486	1.441	1.451
μ, mm^{-1}	2.72	2.22	2.24
T, °C	22(2)	22(2)	22(2)
radiation		Zr-filtered Mo Kα, $\lambda = 0.710\ 69$ Å	
2θ range, deg	3−37	3−40	3−32
index ranges	$-9 \leq h \leq +9$	$-10 \leq h \leq +12$	$-8 \leq h \leq +9$
	$0 \leq k \leq 11$	$0 \leq k \leq 13$	$0 \leq k \leq 10$
	$-15 \leq l \leq +15$	$-17 \leq l \leq +18$	$-14 \leq l \leq +14$
scan type	$\theta/2\theta$	$\theta/2\theta$	$\theta/2\theta$
no. of reflcns collcd	3447	5332	2317
no. of unique reflcns with $(I > 2.5\sigma(I))$	2876	4326	2221
transm factors			
min	0.778	0.662	0.507
max	0.970	0.665	0.939
no. of params	551	695	154
goodness-of-fit[a]	1.07	1.83	4.67
R[b]	0.035	0.034	0.106
R_w	0.064[c]	0.061[c]	0.111[d]
deepest hole/highest peak in diff Fourier map, e Å^3	−0.520/0.670	−0.480/0.600	−0.990/1.400

[a] Goodness-of-fit = $[\sum[w(F_o^2 - F_c^2)^2]/(M - N)]^{1/2}$, where M is the number of reflections and N is the number of parameters refined. [b] $R = \sum||F_o| - |F_c||/\sum|F_o|$. [c] $R_w = [\sum[w(F_o^2 - F_c^2)^2]/\sum[w(F_o^2)^2]]^{1/2}$. [d] $R_w = \sum[w^{1/2}|(F_o - F_c)|]/\sum[w^{1/2}|F_o|]$.

substituting the mixed nitrile/isocyanide ligand, NCC_6H_4NC, for CNC_6H_4NC. The dark red compound was further purified by recrystallization from 1:2 toluene/hexane (29% yield). Anal. Calcd for $C_{68}H_{56}N_4P_4W$: C, 66.03; H, 4.56; N, 4.53. Found: C, 66.08; H, 5.14; N, 4.46. ^{31}P NMR δ(ppm): 31.3, 47.4 d. IR (cm^{-1}): ν_{CN}, 2212 s; ν_{NC}, 1951 s.

X-ray Structural Determination of $W(N_2)_2(DPPE)_2$. Crystallographic and other experimental data are summarized in Table 1. Crystals were obtained fortuitously as a product of the initial crystallization of *cis*-$(CNC_6H_4NC)_2W(DPPE)_2$. An orange crystal of $W(N_2)_2$-$(DPPE)_2$ with dimensions $0.30 \times 0.15 \times 0.10$ mm was mounted and sealed in a quartz capillary tube with epoxy. Empirical absorption corrections were made on the data set.[6] Data were sorted and collected using PCXTL.[4] Orientation and crystal decay were monitored by measuring the intensities of three reference reflections at intervals of 120 minutes. Minimal intensity losses were observed. Data reduction, handling, and analysis were performed using NRCVAX.[7] The locations of the tungsten and phosphorus atoms were determined by direct methods using SHELXS-86.[8] The remaining non-hydrogen atoms were located using a combination of tangent expansion and difference Fourier techniques. The structure was refined against F^2 using SHELXL-93.[9] All heavy atoms were refined anisotropically. Hydrogen atoms were allowed to ride on the heavy atom to which they were attached, with hydrogen atom thermal parameters fixed at 1.5 times the equivalent isotropic thermal parameter of the heavy atom. Neutral atom scattering factors were used for all atoms.[10] Weights based on counting statistics were used in the final stages of refinement. Structural drawings were made using ORTEP[11] and PLUTO.[12]

(6) Flack, H. D. *Acta Crystallogr.* **1974**, *A30*, 569.
(7) Gabe, E. J.; Le Page, Y.; Charland, J-P.; Lee, F. L.; White, P. S. *J. Appl. Crystallogr.* **1989**, *22*, 384.
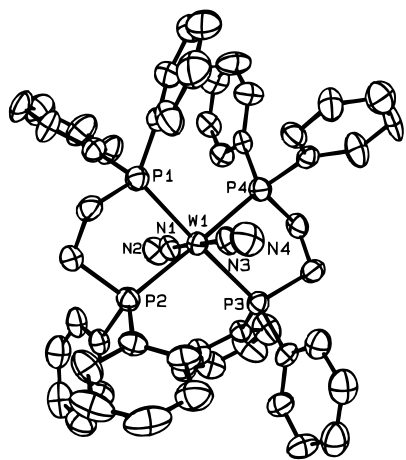(8) Sheldrick, G. M. *Acta Crystallogr.* **1990**, *A46*, 467.
(9) Sheldrick, G. M. *J. Appl. Crystallogr.*, manuscript in preparation.
(10) *International Tables for Crystallography*; Wilson, A. J. C., Ed.; Kluwer Academic Publishers: Dordrecht, The Netherlands, 1992; Vol. C, Table 6.1.1.3, pp 500−502.
(11) Johnson, C. K. ORTEP II. Report ORNL-5138; (Oak Ridge National Laboratory: Oak Ridge, TN, 1976.

X-ray Structural Determination of $(CNC_6H_4NC)_2W(DPPE)_2$. Crystallographic and other experimental data are summarized in Table 1. Dark red crystals were obtained by slow evaporation of a saturated solution in 1:2 toluene/hexane overnight. The crystals were extraordinarily stable in air. A suitable crystal with the dimensions $0.3 \times 0.25 \times 0.15$ mm was sealed in a quartz capillary tube and used for data collection. Data collection, structural solution, and refinement were identical to that for $W(N_2)_2(DPPE)_2$.

X-ray Structural Determination of $(NCC_6H_4NC)_2W(DPPE)_2$. Crystallographic and other experimental data are summarized in Table 1. Dark red crystals were obtained by slow evaporation of a saturated solution as previously described for *cis*-$(CNC_6H_4NC)_2W(DPPE)_2$. The crystals grew as thin plates, most of which were unsuitable for data collection. Again, the crystals were air-stable. A marginally suitable crystal with the dimensions $0.3 \times 0.2 \times 0.05$ mm was sealed in a quartz capillary tube and used for data collection. Empirical absorption corrections were made on the data set.[6] Unlike the crystals for *cis*-$(CNC_6H_4NC)_2W(DPPE)_2$, crystals for *cis*-$(NCC_6H_4NC)_2W(DPPE)_2$ diffracted rather poorly, exhibiting broad asymmetric intensity peaks. In addition, the large range in transmission factors (0.570−0.939, averaging 0.712) indicates absorption problems in the data. Several crystals were analyzed, and two complete separate data sets were collected in order to obtain the less than optimal structure reported here. The structure solved easily with the exception of the location of one NCC_6H_4NC ligand, which appeared to exhibit some degree of disorder. Attempts to model this disorder by assigning partial occupancy to two orientations of the ligand were unsuccessful. Isotropic refinement of the structure resulted in chemically unreasonable distortions of this ligand. In order to avoid an unreasonable geometry the aromatic ring and nitrile group for this ligand were refined as a rigid idealized group. Importantly, the W−C−N−C atoms were allowed to refine freely; thus there were no constraints on the CNC angle for this ligand. All phenyl groups in the molecule were refined as rigid groups. Anisotropic refinement resulted in unusually large thermal ellipsoids for a number of terminal atoms. Since it was unclear whether this

(12) Motherwell, S. PLUTO84. University Chemical Laboratory Cambridge, U.K., 1984.

Figure 1. Solid state structure of W(N₂)₂(DPPE)₂. Thermal ellipsoids are plotted at the 35% probability level. Hydrogen atoms are omitted for clarity.

was the result of disorder, dynamic motion in the lattice, or poor data (despite similar solutions from two data sets), we elected to restrict anisotropic refinement to the tungsten and phosphorus atoms. Although the quality of this structure is somewhat less than ideal, the geometric parameters of the structure relating to the work described here are clearly evident. General solution and refinement parameters were identical to those from *cis*-(CNC₆H₄NC)₂W(DPPE)₂, except that the structure was refined against F rather than F^2 using SHELX-76.[13]

Results and Discussion

Structure of W(N₂)₂(DPPE)₂. Although the structure of W(N₂)₂(DPPE)₂ has not been reported, the crystal structure of its molybdenum analog revealed four coordinated phosphorus atoms in a planar configuration, with the dinitrogen ligands *trans* to one another, giving the structure local D_{4h} symmetry.[14] This geometry would appear to minimize steric repulsions between phenyl rings of the phosphine ligands, but is probably not favored geometry based on electronic considerations. This is borne out in the structure of W(N₂)₂(PMe₂Ph)₄.[15] With smaller groups bonded to phosphorus the structure adopts the *cis* configuration. In this configuration the dinitrogen ligands are able to withdraw more dπ electron density from the metal center than when *trans* to a phosphine. The metal center is certain to be electron rich as a result of the coordination of four strong σ donors; adoption of the *cis* geometry would serve to lower electron–electron repulsion at the metal center.

During the recrystallization process in the initial purification of *cis*-(CNC₆H₄NC)₂W(DPPE)₂, a few orange crystals were isolated among the deep red crystals of the predominant product. These crystals were the same color as the starting material, but exhibited a different crystal habit from the very thin plates which formed during attempts to grow single crystals of W(N₂)₂-(DPPE)₂. A subsequent structural determination revealed the molecule shown in Figure 1. Positional parameters and equivalent isotropic thermal parameters are given in Table 2. Selected bond lengths and angles are given in Table 3. The structure differs somewhat from the molybdenum analog, which is rigorously centrosymmetric in the solid state, with the Mo atom lying on a crystallographic inversion center. The tungsten complex is not constrained in this manner. The average N≡N bond length is 1.133 Å, compared with 1.118 Å in Mo(N₂)₂-(DPPE)₂, indicating that there is more electron density on

(13) Sheldrick, G. M. A Program for Crystal Structure Solution. Institute fur Anorganische Chemie der Universität, Gottingen, Germany, 1976.

(14) Uchida, T.; Uchida, Y.; Hidai, M.; Kodama, T. *Acta Crystallogr.* **1975**, *B31*, 1197.

(15) Dadkhah, H.; Dilworth, J. R.; Fairman, K.; Kan, C.; Richards, R. L. *J. Chem. Soc., Dalton Trans.* **1985**, 1523.

Table 2. Atomic Coordinates ($\times 10^4$) and Equivalent Isotropic Displacement Parameters ($\text{Å}^2 \times 10^3$) for W(N₂)₂(DPPE)₂

	x	y	z	$U_{\text{iso}}{}^a$
W1	2339(0)	1630(0)	2476(0)	48(0)
P1	3027(3)	2847(2)	1463(1)	58(2)
P2	3084(2)	285(2)	1415(1)	55(2)
P3	1569(2)	480(2)	3511(1)	55(2)
P4	1662(2)	2996(2)	3510(1)	55(2)
N1	4029(9)	1235(7)	2824(5)	66(7)
N2	4976(10)	998(8)	3026(6)	83(8)
N3	659(9)	1974(7)	2125(5)	69(7)
N4	−304(10)	2167(8)	1921(6)	92(9)
C1	2069(12)	4177(9)	1330(6)	56(8)
C7	4597(11)	3240(9)	1328(8)	63(8)
C15	1985(12)	−358(8)	973(7)	59(9)
C21	4323(11)	−904(10)	1475(5)	53(9)
C27	2801(10)	−449(8)	3925(7)	51(8)
C33	370(11)	−370(11)	3437(5)	53(8)
C41	109(10)	3917(8)	3577(8)	50(8)
C47	2680(11)	3955(10)	3700(5)	52(8)
C2	990(16)	4256(12)	969(6)	90(11)
C3	183(17)	5260(17)	956(8)	115(14)
C4	400(21)	6172(17)	1247(11)	131(17)
C5	1435(19)	6133(15)	1600(10)	114(15)
C6	2262(13)	5133(14)	1621(7)	91(10)
C8	5226(14)	3244(10)	1971(7)	88(11)
C9	6400(16)	3556(11)	1902(9)	108(13)
C10	6953(14)	3866(12)	1226(11)	107(13)
C11	6373(15)	3897(11)	600(9)	100(12)
C12	5200(14)	3583(10)	652(7)	85(10)
C16	2240(12)	−831(9)	233(7)	84(10)
C17	1363(17)	−1304(10)	−72(8)	96(12)
C18	203(16)	−1312(11)	354(11)	99(14)
C19	−64(14)	−865(12)	1084(9)	95(12)
C20	815(14)	−390(9)	1376(6)	69(9)
C22	4143(11)	−1983(12)	1464(6)	67(9)
C23	5085(18)	−2873(11)	1537(6)	91(12)
C24	6275(15)	−2714(15)	1630(7)	95(13)
C25	6495(14)	−1663(16)	1640(7)	91(13)
C26	5545(15)	−760(11)	1571(6)	74(11)
C28	2919(13)	−469(10)	4704(7)	96(11)
C29	3940(18)	−1124(12)	4958(8)	127(14)
C30	4831(13)	−1782(11)	4462(10)	98(12)
C31	4722(13)	−1781(10)	3704(8)	81(10)
C32	3718(12)	−1112(10)	3455(6)	66(9)
C34	−842(14)	154(10)	3304(6)	73(10)
C35	−1769(12)	−467(14)	3230(6)	83(11)
C36	−1527(14)	−1587(14)	3281(7)	88(13)
C37	−353(16)	−2097(10)	3396(7)	87(11)
C38	574(11)	−1490(11)	3480(5)	68(9)
C42	−279(12)	4343(9)	2915(7)	66(10)
C43	−1399(14)	5084(11)	2931(7)	77(10)
C44	−2144(13)	5409(11)	3579(10)	90(12)
C45	−1809(13)	4986(12)	4247(8)	102(12)
C46	−680(14)	4256(11)	4246(7)	89(11)
C48	3852(13)	3535(9)	3926(6)	68(9)
C49	4684(12)	4199(13)	4067(6)	73(10)
C50	4371(14)	5304(13)	3982(7)	92(12)
C51	3254(16)	5735(10)	3751(8)	104(12)
C52	2400(11)	5080(11)	3618(6)	76(10)
C13	3062(10)	2143(8)	548(5)	65(8)
C14	3820(10)	994(8)	596(5)	68(8)
C39	755(10)	1354(8)	4329(5)	68(8)
C40	1509(10)	2255(8)	4422(5)	65(8)

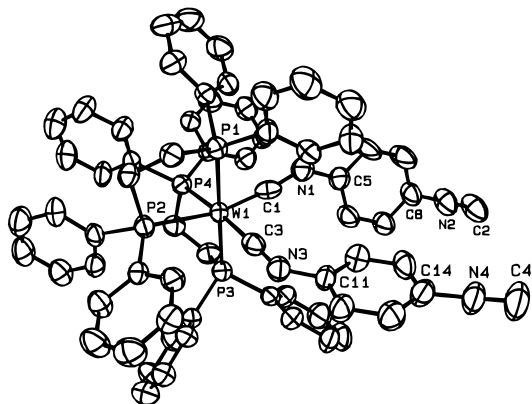^{a} U_{iso} is defined as one-third of the trace of the orthogonalized $\mathbf{U}_{ij}$ tensor.

tungsten available for back-donation. In spite of this, W(N₂)₂-(DPPE)₂ retains the *trans* geometry, indicating that ligand–ligand repulsions are the determinative factor in establishing the structure of the molecule.

Structures of (CNC₆H₄NC)₂W(DPPE)₂ and (NCC₆H₄-NC)₂W(DPPE)₂. A perspective drawing of *cis*-(CNC₆H₄-NC)₂W(DPPE)₂ is shown in Figure 2. Final positional and thermal parameters are included in Table 4; selected bond lengths and angles are given in Table 5. It is immediately

Figure 2. Solid state structure of *cis*-(CNC$_6$H$_4$NC)$_2$W(DPPE)$_2$. Thermal ellipsoids are plotted at the 35% probability level. Hydrogen atoms are omitted for clarity.

Table 3. Selected Bond Lengths (Å) and Angles (deg) for W(N$_2$)$_2$(DPPE)$_2$

	Bond Lengths		
W1−P1	2.452(3)	P2−C14	1.846(10)
W1−P2	2.466(3)	P3−C27	1.832(12)
W1−P3	2.455(3)	P3−C33	1.839(15)
W1−P4	2.444(3)	P3−C39	1.832(10)
W1−N1	1.996(11)	P4−C41	1.846(10)
W1−N3	1.985(10)	P4−C47	1.829(14)
P1−C1	1.814(12)	P4−C40	1.850(10)
P1−C7	1.842(13)	N1−N2	1.126(15)
P1−C13	1.839(10)	N3−N4	1.141(16)
P2−C15	1.818(15)	C13−C14	1.517(13)
P2−C21	1.821(12)	C39−C40	1.523(16)

	Bond Angles		
P1−W1−P2	80.06(10)	P3−W1−P4	79.62(10)
P1−W1−P3	177.34(9)	P3−W1−N1	86.8(3)
P1−W1−P4	98.30(10)	P3−W1−N3	92.3(3)
P1−W1−N1	94.9(3)	P4−W1−N1	90.0(3)
P1−W1−N3	86.1(3)	P4−W1−N3	91.3(3)
P2−W1−P3	102.05(10)	N1−W1−N3	178.2(4)
P2−W1−P4	178.00(11)	W1−N1−N2	178.9(10)
P2−W1−N1	89.0(3)	W1−N3−N4	179.6(9)
P2−W1−N3	89.8(3)		

apparent that the substitution of the dinitrogen ligands with isocyanides has significantly altered the electronic environment of the tungsten metal center. The adoption of the *cis* configuration indicates that the replacement of the very weak dinitrogen bases with much stronger σ donors has increased the charge density at the metal center to a point where the need to lower electron−electron repulsion at the metal supersedes the effects of ligand−ligand repulsion.

Isocyanide ligands are usually only moderately capable π acceptors, at least when competing with carbon monoxide for π density.[16] This is true even when there are phosphine ligands in the coordination sphere, as in the complex W(CO)$_4$-(PPh$_3$)CNC$_6$H$_4$NCW(CO)$_4$(PPh$_3$).[17] Perhaps the most dramatic features in the *cis*-(CNC$_6$H$_4$NC)$_2$W(DPPE)$_2$ structure are the extraordinary CNC bond angles, 136.8(11) and 141.4(8)°, in the coordinated isocyanide groups bonded to tungsten. In contrast, the CNC angles on the "free" ends of the ligands are 178.4(14)° and 174.5(14)°. Figure 3 compares bond lengths and angles in a coordinated isocyanide in *cis*-(CNC$_6$H$_4$NC)$_2$W-(DPPE)$_2$ with a more typical coordination geometry in (W(CO)$_4$-(PPh$_3$)CNC$_6$H$_4$NCW(CO)$_4$(PPh$_3$). Bends similar to those in (CNC$_6$H$_4$NC)$_2$W(DPPE)$_2$ have been observed in *aliphatic* isocyanides coordinated to electron-saturated metal centers.

(16) Guy, M. P.; Guy, J. T.; Bennett, D. W. *J. Mol. Struct.: THEOCHEM* **1985**, *122*, 95.
(17) Rommel, J. S.; Weinrach, J. B.; Grubisha, D. S.; Bennett, D. W. *Inorg. Chem.* **1988**, *27*, 2945.

Table 4. Atomic Coordinates (×10^4) and Equivalent Isotropic Displacement Parameters (Å^2 × 10^3) for (CNC$_6$H$_4$NC)$_2$W(DPPE)$_2$

	x	y	z	U$_{iso}$[a]
W1	1576(0)	3124(0)	2579(0)	54(0)
P1	1802(2)	4447(1)	3184(1)	62(1)
P2	−547(2)	3947(1)	3474(1)	62(1)
P3	1369(2)	1772(1)	1997(1)	64(1)
P4	836(2)	4275(1)	1481(1)	62(1)
N1	4267(7)	2719(6)	1703(4)	83(7)
N2	8594(8)	−425(7)	326(5)	107(8)
N3	2591(6)	1263(6)	3734(4)	75(6)
N4	6937(8)	−1702(6)	4142(5)	107(8)
C1	3137(9)	2824(6)	2012(4)	74(8)
C2	9516(10)	−1089(10)	79(6)	125(11)
C3	2183(8)	2033(7)	3276(5)	70(7)
C4	7826(10)	−2233(9)	4267(7)	134(12)
C29	549(6)	4902(6)	4005(4)	68(7)
C30	−632(7)	5130(6)	3863(4)	67(6)
C55	1196(8)	2281(6)	1075(4)	79(8)
C56	363(7)	3477(6)	1069(4)	75(7)
C5	5332(9)	1929(8)	1320(5)	75(8)
C6	6359(10)	2126(9)	1057(7)	147(13)
C7	7443(9)	1343(10)	713(6)	136(12)
C8	7504(9)	368(9)	637(5)	86(9)
C9	6488(9)	157(8)	860(5)	88(9)
C10	5415(8)	933(9)	1200(5)	82(9)
C11	3670(8)	484(7)	3845(5)	67(8)
C12	4721(10)	325(7)	3267(5)	83(9)
C13	5800(8)	−412(8)	3378(6)	85(9)
C14	5821(10)	−998(8)	4050(7)	86(10)
C15	4793(11)	−876(9)	4579(6)	100(10)
C16	3712(9)	−142(8)	4486(5)	88(9)
C17	3056(8)	4045(8)	3589(5)	67(7)
C18	4007(9)	3092(8)	3433(5)	77(9)
C19	4953(9)	2784(8)	3759(6)	97(10)
C20	4916(10)	3426(10)	4240(6)	100(12)
C21	3963(11)	4386(10)	4387(6)	106(12)
C22	3051(9)	4711(8)	4069(5)	89(9)
C23	1894(8)	5703(7)	2658(5)	62(8)
C24	2676(8)	5634(7)	1943(6)	79(9)
C25	2751(9)	6543(10)	1492(6)	101(11)
C26	2037(12)	7547(10)	1751(7)	111(13)
C27	1297(10)	7643(8)	2454(7)	99(11)
C28	1212(8)	6738(8)	2910(5)	85(9)
C31	−1922(7)	4505(8)	3194(4)	65(7)
C32	−2152(8)	3884(7)	2811(4)	72(8)
C33	−3203(10)	4262(9)	2619(5)	91(10)
C34	−4069(10)	5273(10)	2798(6)	103(11)
C35	−3855(10)	5896(9)	3177(6)	109(11)
C36	−2794(9)	5529(8)	3372(5)	87(9)
C37	−980(8)	3152(6)	4334(4)	58(7)
C38	−167(8)	2601(7)	4741(5)	67(8)
C39	−468(9)	1990(7)	5392(5)	80(9)
C40	−1571(11)	1928(8)	5643(5)	99(11)
C41	−2382(8)	2487(8)	5260(5)	96(10)
C42	−2099(8)	3096(7)	4605(5)	81(8)
C43	2606(7)	438(7)	1811(6)	68(8)
C44	3170(9)	57(8)	1100(6)	91(10)
C45	4087(11)	−968(10)	994(7)	115(12)
C46	4423(10)	−1625(10)	1577(8)	113(12)
C47	3875(10)	−1276(8)	2289(7)	109(12)
C48	2956(8)	−243(8)	2402(5)	86(9)
C49	170(7)	1267(6)	2470(5)	65(7)
C50	−112(8)	1077(6)	3238(5)	73(8)
C51	−977(9)	690(7)	3635(5)	85(9)
C52	−1607(10)	473(9)	3271(7)	110(11)
C53	−1380(9)	657(8)	2513(7)	110(12)
C54	−484(9)	1034(7)	2097(5)	93(10)
C57	−449(7)	5579(7)	1575(4)	58(7)
C58	−1387(9)	5801(8)	1293(5)	88(8)
C59	−2319(9)	6800(10)	1385(6)	107(11)
C60	−2376(10)	7583(9)	1770(6)	113(11)
C61	−1431(10)	7354(8)	2039(5)	100(10)
C62	−490(8)	6364(8)	1945(5)	81(8)
C63	1905(8)	4597(7)	657(4)	59(7)
C64	3022(9)	3821(7)	388(5)	80(9)
C65	3837(9)	4020(8)	−237(6)	94(9)
C66	3575(10)	5004(10)	−596(5)	105(11)
C67	2454(11)	5810(9)	−353(6)	107(11)
C68	1644(8)	5608(7)	270(5)	82(8)

[a] U$_{iso}$ is defined as one-third of the trace of the orthogonalized **U**$_{ij}$ tensor.
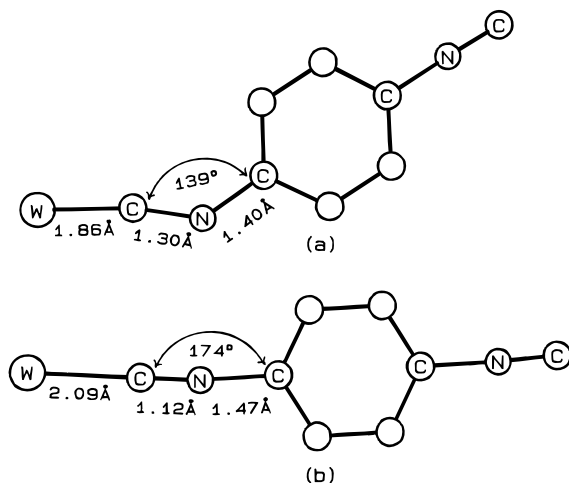
Figure 3. (a) Average bond lengths and angles in an aromatic isocyanide ligand coordinated to tungsten in *cis*-(CNC$_6$H$_4$NC)$_2$W-(DPPE)$_2$, illustrating the extraordinary C−N−C bend, very short W−C distance, and elongated C−N bond. (b) Comparative bond lengths and angles in a typical aromatic tungsten isocyanide complex, W(CO)$_4$-(PPh$_3$)CNC$_6$H$_4$NCW(CO)$_4$(PPh$_3$).

Table 5. Selected Bond Lengths (Å) and Angles (deg) for (CNC$_6$H$_4$NC)$_2$W(DPPE)$_2$

Bond Lengths			
W1−P1	2.471(3)	N1−C5	1.403(11)
W1−P2	2.5884(21)	N2−C2	1.157(12)
W1−P3	2.463(3)	N2−C8	1.381(12)
W1−P4	2.561(3)	N3−C3	1.277(11)
W1−C1	1.846(10)	N3−C11	1.402(12)
W1−C3	1.882(9)	N4−C4	1.143(16)
N1−C1	1.329(15)	N4−C14	1.400(15)

Bond Angles			
P1−W1−P2	78.97(9)	P3−W1−C3	89.4(4)
P1−W1−P3	178.70(8)	P4−W1−C1	90.2(3)
P1−W1−P4	102.24(9)	P4−W1−C3	168.0(4)
P1−W1−C1	86.6(4)	C1−W1−C3	87.3(4)
P1−W1−C3	89.3(4)	C1−N1−C5	136.8(11)
P2−W1−P3	101.18(9)	C2−N2−C8	178.4(14)
P2−W1−P4	90.36(7)	C3−N3−C11	141.4(8)
P2−W1−C1	165.4(4)	C4−N4−C14	174.5(14)
P2−W1−C3	95.0(3)	W1−C1−N1	168.6(10)
P3−W1−P4	79.05(9)	W1−C3−N3	177.5(10)
P3−W1−C1	93.3(4)		

Table 6. GNC Angles of Isocyanide Complexes

complex	FOS[d]	angle, deg	ref
trans-[Mo(CNMe)$_2$(DPPE)$_2$]	0	156	27
Ru(*t*-BuNC)$_4$(PPh$_3$)[a]	0	130	19
Fe(*t*-BuNC)$_5$[b]	0	135	19
Co$_2$(*t*-BuNC)$_8$	0	154	28
mer-ReCl(N$_2$)(CNMe)(P(OMe)$_3$)$_3$	+1	169	30
mer-[Cr(NO)(*t*-BuNC)$_3$(DPPM)]PF$_6$[c]	+1	176	31
MoCl$_2$(*t*-BuNC)(CO)(PMe$_3$)$_3$	+2	178	32
[(*t*-BuNC)$_6$MoBr]Br	+2	173	33
(*t*-BuNC)$_3$W(CO)$_2$I$_2$	+2	173	34
Nb$_2$Cl$_6$(*t*-BuNC)$_6$	+3	175	35
Ta$_2$Cl$_6$(*t*-BuNC)$_6$	+3	176	35
Cr(CNC$_6$H$_5$)$_6$	0	173	20
(CO)$_4$W(C(OCH$_3$)(C$_6$H$_5$))(CNC$_6$H$_4$-*p*-CH$_3$)	0	178	21
(CO)$_4$W(C(OCH$_3$)(C$_6$H$_5$))(*t*-BuCN)	0	172	21
W(CO)$_4$(PPh$_3$)CNC$_6$H$_4$NCW(CO)$_4$(PPh$_3$)	0	176	17
W(CO)$_4$(PEt$_3$)CNC$_6$H$_4$NCW(CO)$_4$(PEt$_3$)	0	169	17

[a] The mean value of C≡N−C angles of the two equatorial *t*-BuCN ligands. [b] The mean value of C≡C angles of two of the radial isocyanide ligands. [c] DPPM = 1,2-bis(dimethylphosphino)ethane. [d] FOS = Formal oxidation state.

Table 6 is a compilation of CNC bond angles taken from the literature, along with the formal oxidation state of the metal. From this comparison it is clear that significant deviations from linearity occur only when the isocyanide ligands are aliphatic and when the transition metal is in a zero oxidation state and not bonded to π-accepting ligands. Aliphatic isocyanides tend to behave as π acids only when there are no other ligands competing for dπ electron density. In such cases, unlike their aromatic counterparts, the electron density remains localized on the nitrogen atom in the isocyanide group, and pairing effects tend to force the structure from linearity toward a trigonal configuration (i.e., sp to sp^2 hybridization).

As indicated in Table 6, much smaller bends are ordinarily observed in aromatic isocyanides. Even in cases where the aromatic isocyanide is a μ-bridging ligand and the remaining ligands are strong electron donors such as η^5-C$_5$H$_5$,[18] the CNC angle is greater than 160°. Note that the zerovalent transition metal surrounded completely by aliphatic isocyanides in [Fe-(*t*-BuNC)$_5$] produces bends of 135° in two of the five isocyanides,[19] while the others remain approximately linear. In contrast, even when the metal is coordinated exclusively by aromatic isocyanides, as in Cr(CNC$_6$H$_5$)$_6$, the isocyanides exhibit very little deviation from linearity.[20] Aryl isocyanides are reasonable π acceptors, due in large part to their ability to delocalize charge away from the nitrogen atom on the isocyanide into the ring. Thus significant CNC bending would be expected only when there is so much excess charge density at the metal that the aromatic rings on the isocyanide ligands can no longer accommodate the excess charge in the dπ−pπ system.[1]

The extent of electron saturation on tungsten in *cis*-(CNC$_6$H$_4$-NC)$_2$W(DPPE)$_2$ is underscored by significant changes in W−C and C−N bond lengths. In general, these bond lengths change very little when free isocyanides coordinate to metal centers, despite significant changes in spectroscopic measurements such as C−N stretching frequencies.[21] This is the case even for the series [Cr(CNPh)$_6$]$^{n+}$, (n = 1, 2, 3), in which only slight changes occur in W−C and C−N internuclear distances as the metal becomes increasingly oxidized.[22] In W(CO)$_4$(PPh$_3$)CNC$_6$H$_4$-NCW(CO)$_4$(PPh$_3$), the W−C and C−N bond lengths are 2.084-(11) and 1.134(12) Å, respectively. The comparative C−N distance in CNC$_6$H$_4$NC is 1.166(4) Å.[23] In *cis*-(CNC$_6$H$_4$-NC)$_2$W(DPPE)$_2$ the average W−C bond length is 1.86(1) Å, over 0.2 Å shorter than in W(CO)$_4$(PPh$_3$)CNC$_6$H$_4$NCW(CO)$_4$-(PPh$_3$). This is very close to the W≡C internuclear distance of 1.88 Å, reported for the carbyne complex I(CO)$_4$W≡CC$_6$H$_5$.[24] The average C−N distance for the coordinated end of the isocyanide ligands is 1.30(2) Å, 0.17 Å longer than in the carbonyl isocyanide complex and 0.14 Å longer than that in the free ligand. Rarely are such dramatic changes observed! These major perturbations are clear evidence that the tungsten is virtually saturated with electron density in *cis*-(CNC$_6$H$_4$-NC)$_2$W(DPPE)$_2$.

When the diisocyanide ligands are replaced by mixed nitrile/isocyanide ligands, the structure of the molecule, *cis*-(NCC$_6$H$_4$-NC)$_2$W(DPPE)$_2$ is nearly identical to the complex containing the diisocyanide ligands. Despite the relatively poor quality of the structure, the main features parallel those of (CNC$_6$H$_4$-NC)$_2$W(DPPE)$_2$. The mean CNC angle is 133°, and the average W−C and C−N distances are 1.86 and 1.30 Å, respectively. Both molecules contain ligands with available lone pairs which

(18) Tanase, T.; Fukushima, T.; Nomura, T.; Yamamoto, Y. *Inorg. Chem.* **1994**, *33*, 32.
(19) Basset, J.; Berry, D. E.; Barker, G. K.; Green, M. *J. Chem. Soc., Dalton Trans.* **1979**, 1003.
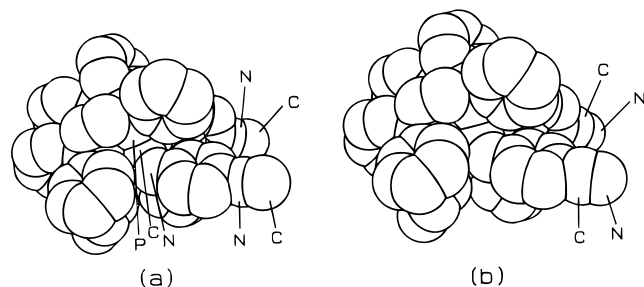(20) Ljungstrom, E. *Acta Chem. Scand.* **1978**, *A32*, 47.
(21) Guy, M. P.; Guy, J. T.; Bennett, D. W. *Organometallics* **1986**, *5*, 1696.
(22) Hahn, E. F.; Tamm, M. *Chem. Ber.* **1992**, *125*, 119.
(23) Colapietro, M.; Domenicano, A.; Portalone, G.; Torrini, I.; Hargittai, I.; Schultz, G. *J. Mol. Struct.* **1984**, *125*, 19.
(24) Fischer, E. O.; Kreis, G.; Kreiter, C. G.; Müller, J.; Huttner, G.; Lorenz, H. *Angew. Chem., Int. Ed. Engl.* **1973**, *12*, 564.

Figure 4. Space-filling drawings of (a) *cis*-(CNC$_6$H$_4$NC)$_2$W(DPPE)$_2$ and (b) *cis*-(NCC$_6$H$_4$NC)$_2$W(DPPE)$_2$ illustrating the confining coordination environment of tungsten in both molecules. The tungsten atom is not visible from any perspective in either molecule. Orientations of both molecules are the same as in Figure 2.

can coordinate to other transition metal complexes. The isocyanide functional groups can bind both low-valent and high-valent transition metals, while the nitrile groups should preferentially coordinate to metals in higher oxidation states.

In light of the excess electron density at the metal, it is quite surprising that these complexes exhibit extraordinary air stability. The lack of susceptibility to atmospheric oxidation must lie in the inaccessibility of the metals in the complexes. Space-filling drawings of both molecules, shown in Figure 4, illustrate graphically that the tungsten atom is completely surrounded by ligands which appear to be sterically constrained about the metal, protecting it from outside attack.

Spectroscopic Studies of *cis*-(RC$_6$H$_4$NC)$_2$W(DPPE)$_2$, R = CN,NC. The ^{31}P NMR spectrum of *cis*-(CNC$_6$H$_4$NC)$_2$W-(DPPE)$_2$ exhibits two doublets, one at 32.3 ppm, $^1J_{WP} = 190$ Hz, $^2J_{PWP} = 5.7$ Hz, and the other at 47.5 ppm, $^1J_{WP} = 269$ Hz, $^2J_{PWP} = 5.7$ Hz. The upfield resonance is assigned to the phosphorus atoms *trans* to the isocyanides; the downfield resonance is assigned to the mutually *trans* phosphorus atoms. A similar pattern is observed in *cis*-W(N$_2$)$_2$(PMe$_2$Ph)$_4$.[25] The

(25) George, T. A.; DeBord, J. R. D.; Kaul, B. B.; Pickett, C. J. *Inorg. Chem.* **1992**, *31*, 1295.
(26) Bailar, J. C., Jr. *J. Inorg. Nucl. Chem.* **1958**, *8*, 165.
(27) Chatt, J.; Pombeiro, A. J. L.; Richards, R. L.; Royston, G. H. D. *J. Chem. Soc., Chem. Commun.* **1975**, 708.
(28) Barker, G. K.; Galas, A. M. R.; Green, M.; Howard, J. A. K.; Stone, F. G. A.; Turney, T. W.; Welch, A. J.; Woodward, P. *J. Chem. Soc., Chem. Commun.* **1977**, 256.
(29) Pombeiro, A. J. L.; Hitchcock, P. B.; Richards, R. L. *J. Chem. Soc., Dalton Trans.* **1987**, 319.
(30) Carvalho, M.; Pombeiro, A. J. L.; Ulrich, S.; Orama, O.; Pickett, C. J.; Richards, R. L. *J. Chem. Soc., Dalton Trans.* **1985**, 2079.
(31) Robinson, W. R.; Wigley, D. E.; Walton, R. A. *Inorg. Chem.* **1985**, *24*, 918.
(32) Carmona, E.; Contreras, L.; Gutierrez-Puebla, E.; Monge, A.; Sanchez, L. *Inorg. Chem.* **1990**, *29*, 700.
(33) Lam, C. T.; Novotny, M.; Lewis, D. L.; Lippard, S. J. *Inorg. Chem.* **1978**, *17*, 2127.
(34) Dreyer, E. B.; Lam, C. T.; Lippard, S. J. *Inorg. Chem.* **1979**, *18*, 1904.
(35) Cotton, F. A.; Duraj, S. A.; Roth, W. J. *J. Am. Chem. Soc.* **1984**, *106*, 6987.

^{31}P NMR spectrum of *cis*-(NCC$_6$H$_4$NC)$_2$W(DPPE)$_2$ is similar to that of the complex containing diisocyanide ligands, with two doublets at 31.3 ppm, $^1J_{PWP} = 181$ Hz, $^2J_{PWP} = 5.6$ Hz, and 47.4 ppm, $^1J_{PWP} = 275$ Hz, $^2J_{PWP} = 5.7$ Hz.

The infrared spectrum of *cis*-(NCC$_6$H$_4$NC)$_2$W(DPPE)$_2$ exhibits only one sharp band of strong intensity in the ν_{CN} (nitrile) stretching region at 2212 cm^{-1}. There is only one discernible band near the ν_{NC} (isocyanide) stretching region as well, a sharp, intense absorption at 1951 cm^{-1}. In the free ligand, CNC$_6$H$_4$-CN, the nitrile stretching frequency is observed at 2233 cm^{-1} and the isocyanide stretching frequency at 2136 cm^{-1}. Thus the isocyanide experiences a 185 cm^{-1} shift to lower frequency, clearly reflecting the increase in charge density from the metal into the π^* molecular orbitals on the ligand. Compare this shift with that for W(CO)$_4$(PPh$_3$)CNC$_6$H$_4$NCW(CO)$_4$(PPh$_3$), with ν_{NC} of 2111 cm^{-1}, a shift of 32 cm^{-1} with respect to uncoordinated CNC$_6$H$_4$NC. Even the "free" end of the ligand experiences a moderate shift to lower frequency of about 21 cm^{-1}. This relatively minor shift indicates clearly that the ligands coordinate through the isocyanide end of the molecule rather than the nitrile end. It appears that the charge perturbation is large enough to delocalize significant electron density throughout the π^* system in the ligand aromatic system, which is also antibonding with respect to the C≡N bond in the nitrile group. The infrared spectrum of *cis*-(CNC$_6$H$_4$NC)$_2$W(DPPE)$_2$ is qualitatively the same, with a sharp, intense band at 2120 cm^{-1}, and another sharp, intense band at 1945 cm^{-1}. The free symmetric ligand, CNC$_6$H$_4$NC, exhibits a ν_{NC} of 2128 cm^{-1}. Thus the coordinated isocyanide experiences a shift of 183 cm^{-1} to lower frequencies, while the uncoordinated isocyanide registers a shift of 8 cm^{-1}.

Conclusions

The complexes synthesized in this work contain electron-rich transition metals surrounded by bulky ligands which appear to insulate the metal from external attack. The diisocyanide and mixed isocyanide/nitrile ligands both project a ligating group into the environment surrounding the complex, providing the potential for coordination with other transition metal centers. The aromatic ring on these ligands allows for charge polarization away from the center of the molecule, providing accessibility to the excess charge through an extended π system. This should make it possible to modulate electron density between two or three transition metals by modifying the ligands on each metal.